Ann. Rep. Fac. Educ., Iwate Univ., Vol. 51 No. 2 (Feb. 1992) 55~63

Time- and Space-Resolved Spectroscopy of Pulsed RF Plasmas in Nitrogen

Nobuyasu SATO* and Yoshiaki KAWASHIMA*

(Received October 15, 1991)

Abstract

An instrumentation for observing time- and space-resolved spectral emissions from a pulsed RF plasma in nitrogen is developed. This provides time and space resolution of 20 ns and 0.5 mm respectively. The observed spectra are the (0, 0) emission line of the first negative system of N_2^+ ions (FNS(0, 0)) and the (0, 0) emission line of the second positive system of N_2 molecules (SPS(0, 0)) at a pressure of 2 Torr. Subsequent progressive changes of the spectra during the RF pulse length are recorded. Information on the electron energy in the gap space for different phases of the RF pulse is obtained by comparing the spectral data with the modeling data.

1. Introduction

In comparison with steady RF plasmas used for many applications in plasma processing, pulsed RF plasmas have some advantages for controlling the electron energy by adjusting the RF pulse shape and pulse duration [1, 2]. Although the pulsed RF plasma has been used recently for plasma processing such as etching silicon with SF_6 [3, 4] and the deposition of amorphous silicon [5, 6], the structure and the associated characteristic of the pulsed RF plasma are not well-known. Consequently, a series of investigations has been initiated in our laboratory to monitor the pulsed RF plasma development in nitrogen.

In the present investigation, highly time resolved techniques involving the use of a photon multiplier and a fast sampling digital oscilloscope are used to monitor the spatio-temporal evolution of the spectral emission from a pulsed RF plasma in nitrogen. The experimental arrangement provides the spectral observation with time and spatial resolution of 20 ns and 0.5 mm respectively. The pulsed RF plasma is generated between parallel plates by an RF potential of a frequency 13.56 MHz, pulse durations of 1-3 microsec and a repetition rate of 500 Hz. The observed spectra are the (0, 0) emission line

* Faculty of Education, Iwate University, Ueda, Morioka 020.

of the first negative system of N_2^+ ions (FNS(0, 0)) and the (0, 0) emission line of the second positive system (SPS(0, 0)) of N_2 molecules. The intensity ratios of these spectral line emissions may provide information about the electron energy distribution in the gap space. In the present experiment, however, the direct measurement of the intensity ratio is difficult, since for this purpose a precise calibration of the optical detecting system is required. Therefore, variations of the electron energy during the development of the pulsed RF plasma are discussed by comparing the observed spectral data with those obtained by a computer modeling.

2. Experimental arrangement and procedure

The experimental arrangement is shown schematically in Fig. 1. Parallel plane electrodes were used with the gap length of 10 mm. The electrodes were made of stainless steel to Harrison profile with overall diameter of 50 mm and are located in a stainless steel vacuum chamber with an internal diameter 15 cm provided with optically flat quartz windows for the observation of RF plasmas. The electrode separation can be changed from outside the chamber by a micrometer adjustment of the position of the lower electrode, which can be located in position to give an accurately known electrode separation of between 0 and 20.0 mm.

The chamber and gas handling manifold were normally evacuated by a mechanical pump (Ulvac GVD-050A) to 5×10^{-3} Torr and flushed with nitrogen of 99.999 purity. The experiment was carried out by flowing the sample gas in the chamber with flowing rates of 10-20 sccm maintaining the gas pressure at 2 Torr. Pressure readings were made using a Pirani gauge calibrated by a Baratron gauge (MKS-122A).

In order to study pulsed RF plasmas, an attempt has been made in the design of the RF power supply to provide a pulse height of more than 500 V, allowing a wide range of pulse repetition frequencies and pulse durations to be achieved. For this purpose, a gated RF pulse oscillator has been designed as shown in Fig. 2. The oscillator produces rectangular

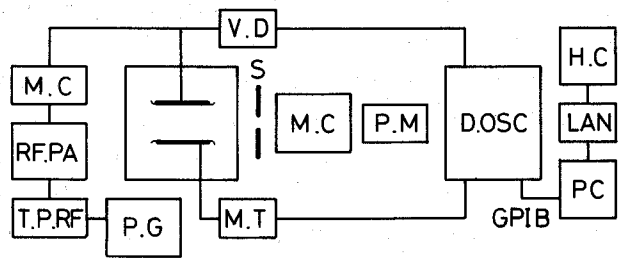

Fig. 1 Experimental arrangement. P.G, pulse generator; T.P.RF, gated RF pulse oscillator; RF.PA, RF power amplifier; M.C, matching circuit; V.D, voltage divider; M.T, matching transformer; S, slit; M.C, monochrometer; P.M, photon multiplier; D.OSC, digital oscilloscope; PC, personal computer; LAN, local area network; H.C, host computer.

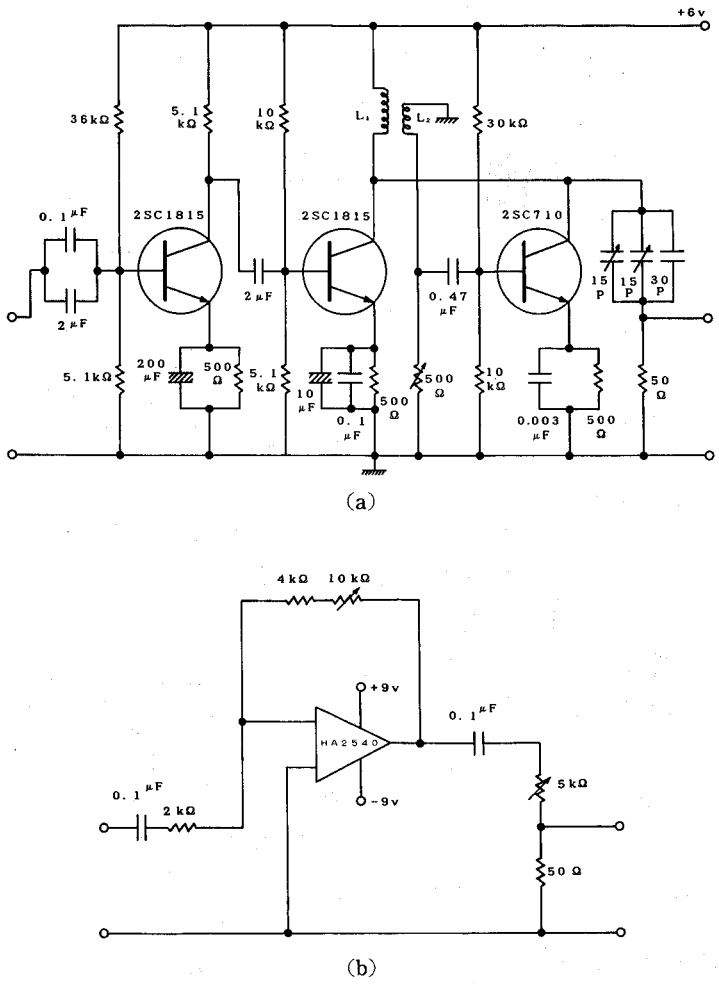

Fig. 2 Gated FR pulse oscillator. (a) is the oscillator circuit and (b) is the wide band preamplifier circuit.

RF voltage pulses of amplitude approximately 10 V peak-to-peak with a rise time of 3-4 cycle of the radio frequency 13.56 MHz. The circuit employed was based on that given by Antokol'ski [7], which was modified to the solid state circuitry. The oscillator was triggered by a pulse generator (PHILIPS PM5715). Fig. 3 shows the input pulse and the output of the gated RF pulse oscillator. The RF pulse was amplified by an RF power amplifier which was a power output unit of a 100 W RF transceiver (YAESU FT-575GX).

The RF power was coupled to the electrode through a matching circuit. The circuitry shown in Fig. 4 is equivalent to a transformer which provides a high RF potential appropriate for initiating and sustaining RF plasmas. With this matching circuit, however, the rectangular RF pulse was modified to a pulse profile with a rise time of 1 microsec and a decay time of about 1.5 microsec. The RF voltage was measured using a capacitive

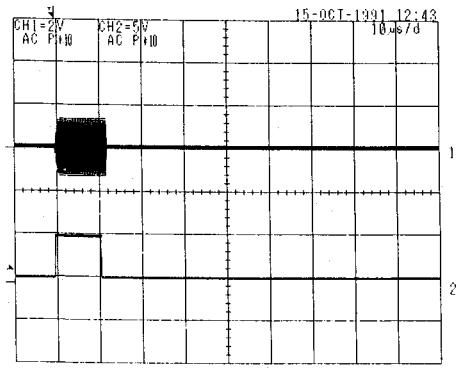

Fig. 3 Output of the gated RF pulse oscillator. Also shown is the trigger pulse in Trace 2.

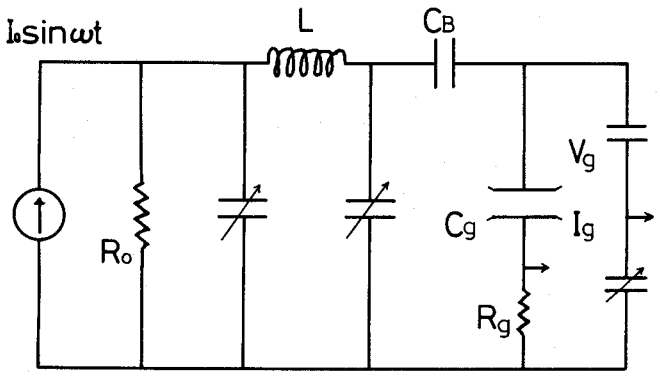

Fig. 4 Matching circuit. R_O, output impedance of the power amplifier; L, coil; C_B, blocking capacitor; C_g, capactiance of the gap; R_g, current detecting resistor.

voltage divider and a digital oscilloscope (Yokogawa DL1200). Fig. 5. shows an RF voltage together with discharge current recorded by the oscilloscope. Care has been taken in the design to ensure adequate high voltage insulation and screening of all RF potentials.

RF plasmas were initiated by irradiation of the electrode surface with UV light from a mercury lamp. After initiation, the plasma was maintained without the UV irradiation. The light emission from the plasma was focused by means of a quartz lens on to the input of a 0.25 m monochrometer (Shimazu SPG-100S) through a 0.1 mm slit with length of 10 cm. This optical arrangement provides a spatial resolution of 0.5 mm. The optical system was mounted on a Z-stage in order to observe spatial variations of the spectral emission in the gap space. Photons from the output of the monochrometer were detected by a photon-multiplier (HAMAMATSU R444). Temporal variations of the photon signal were sampled and averaged by the digital oscilloscope and recorded by a personal computer through a GPIB interface. This photon detecting system has a time constant of about 20 ns for recording the time varying photon signal. It should be noticed, therefore, that the photon emission with a duration less than 20 ns may not be detected correctly by

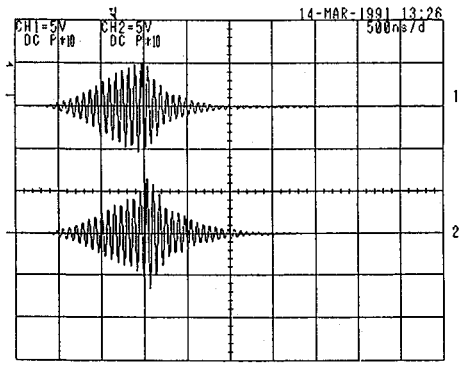

Fig. 5 Profiile of the pulsed RF potential. Trace 1 is the voltage V_g and Trace 2 is the discharge current I_g.

the present system.

The data acquired in the personal computer were transferred to a HITAC M260K computer in Iwate University. Three dimensional displays of the data were made using a software SAS/GRAPH.

3. Results and discussions

The current through the discharge as a function of time is monitored by observing the voltage developed across a 50 Ohm resister connected in series with the discharge gap. As shown in Fig. 6, the discharge current consists of the displacement current and the true current due to motion of the charged species in the gap space. The current increases suddenly around the peak of the voltage pulse, which indicates the initiation of the discharge. At the initiation of the discharge, the current and voltage reach about 1 A and 500 V, respectively, with a phase shift of about 45 degree. This gives rise to a peak

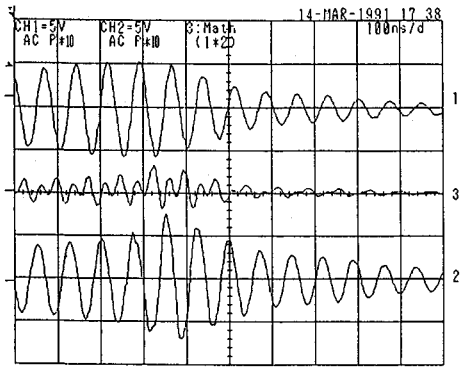

Fig. 6 Time variation of the applied voltage V_g (Trace 1), the discharge current I_g (Trace 3) and the discharge power P (Trace 2).

discharge power of 350 W. The discharge power decreases gradually after the initiation of the discharge. The duration of the discharge in this case is about 2 microsec. The temporal variation of the discharge power is approximately corresponding to that of the total photon flux from the pulsed RF plasma. These observations, however, provide spatially integrated features of the RF plasma. Therefore, spatially resolved observations of the RF plasma are required for investigating the RF plasma structure.

Figs. 7(a) and (b) are respectively the spatio-temporal evolution of the SPS(0, 0) and FNS(0, 0) emissions from the pulsed RF discharge. Significant observations are that at the early stage of the discharge the light emission is most intense and spreads over the gap space, and that in the late stage of the discharge the two small peaks of the emission appear in mid gap and move toward each of the electrodes. These particular variations of the emission associated with the pulsed RF plasma are not observed in the steady RF plasma. It may be expected that the time- and space-dependent variations of the FNS(0, 0) and SPS(0, 0) emissions are different from each other, since the threshold energy of the excited state responsible for FNS(0, 0) emission is much higher than that of SPS(0, 0) emission.

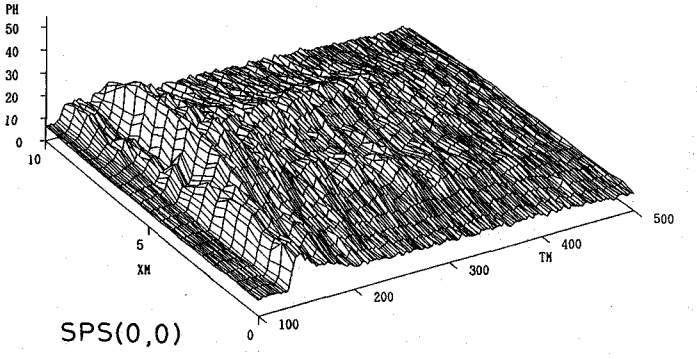

(a)

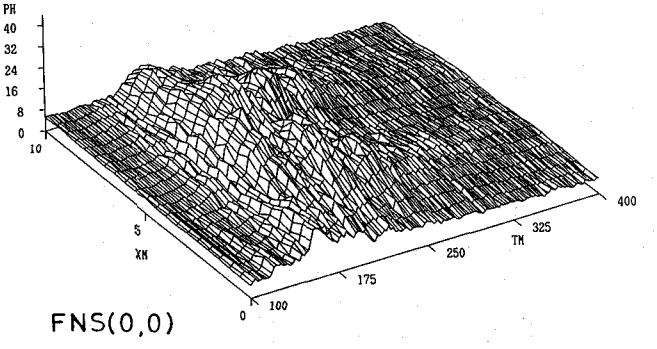

(b)

Fig. 7 Experimentally observed spatio-temporal variations of (a) the SPS(0, 0) emission and (b) the FNS(0, 0) emission.

The difference between the observed distributions of FNS(0, 0) and SPS(0, 0) emissions is so subtle that discussions about the electron energy using the intensity ratio of these emissions may be difficult. Further precise measurements with the calibrated optical detecting system are required for obtaining information on the electron energy experimentally. Consequently, the structure of the pulsed RF plasma such as the distribution of the electron density and the variation of the electron energy is investigated using a computer modeling of the RF plasma [8]. This model includes an electron energy equation in order to take into account non-equilibrium characteristics of the electron transport. The time and spatial variations of the SPS(0, 0) emission calculated using the model, shown in Fig. 8(a), are considerably in good agreement with the experimental observation. This indicates the validity of the present model. Figs. 9(a) and (b) are respectively the electron density distribution and the variation of the electron energy calculated using the model. As shown in these figures, at the early stage of the discharge development, electrons can move through the gap space from one side electrode to the other. This gives rise to heating of the electron throughout the gap space. Because of this, the photon emissions in

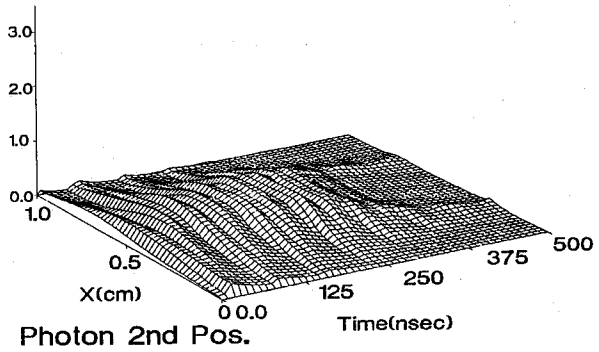

(a)

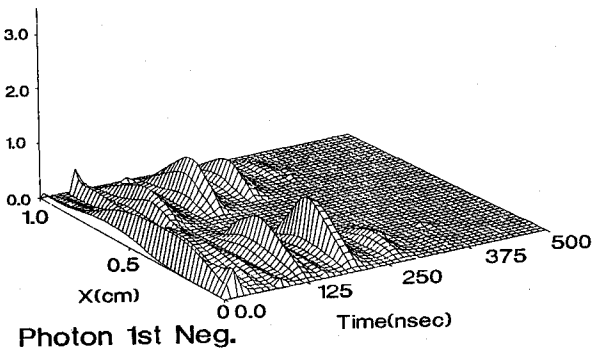

(b)

Fig. 8 Calculated spatio-temporal variations of (a) the SPS(0, 0) emission and (b) the FNS(0, 0) emission.

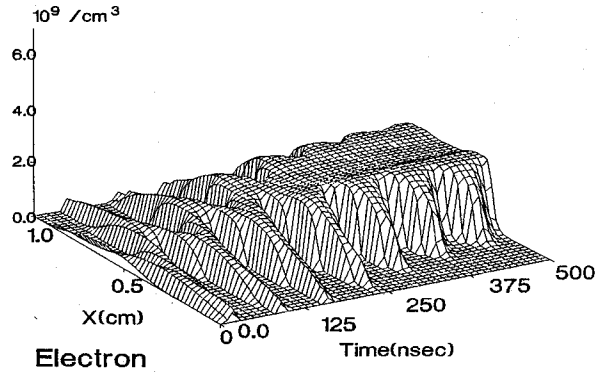

(a)

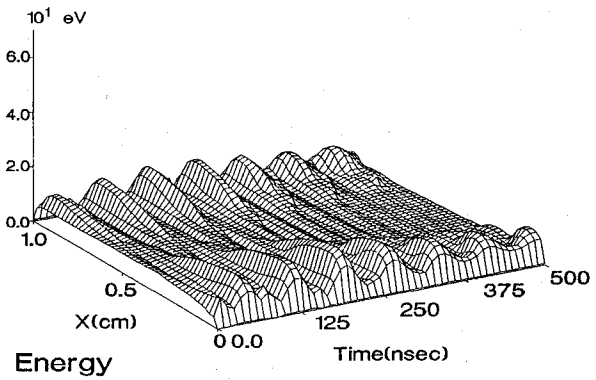

(b)

Fig. 9 Spatio-temporal evolutions of (a) the electron density and (b) the electron energy during the pulsed RF discharge development.

this stage become most intense over the gap space. In the later stage of the discharge development, most of electrons are confined in mid gap. This implies formation of the sheath region in the neighbourhood of the electrodes and of the bulk region in mid gap. In this stage, high energy electrons appear only in the sheath region where the electron density is low enough not to give rise to any observable emission. The light emissions, therefore, are observed only around the boundaries of the bulk region.

As discussed above, the intensity of the spectral emission depends on both the electron density and the electron energy in the plasma. Since the excited state responsible for the FNS(0, 0) emission has a higher threshold energy than that for the SPS(0, 0) emission, the intensity of the FNS(0, 0) emission in both the early and late stages should be decreased in mid gap where the electron energy is considerably low. This is indicated by the calculated FNS(0, 0) emission using the model, as shown in Fig. 8(b). The experimental observation of this emission, shown in Fig. 7(b), is different from the calculated result. This may be caused by the fact that for the present model the life time of the FNS(0, 0) emission is taken

to be 10 ns. If the time duration of the emission is less than 20 ns, the photon detecting system with a time constant of 20 ns may not correctly reproduce the time variation of the photon signal. Further computer treatment of the photon signal such as a deconvolution technique may be required in order to get rid of this problem.

Acknowledgment

The authors wish to acknowledge valuable discussions with Professor S.C. Haydon of The University of New England in Australia in the early stage of this study and with Professor H. Tagashira of Hokkaido University. This research was supported by the Scientific Research Grant of Ministry of Education.

References

[1] N. Sato, *Proc. 1st Australia-Japan Workshop on Gaseous Electronics and Its Applications, Sydney, Australia*, 29-32, (1988)
[2] N. Sato, T. Kamibayashi and H. Tagashira, *Proc. IXth Int. Conf. on Gas Discharges and Their Applications, Venice, Italy*, 633-636, (1988)
[3] R.W. Boswell and D. Henny, *Appl. Phys. Lett.*, **vol. 47**, 1095-1097, (1985)
[4] R.W. Boswell and R.K. Porteou, *J. Appl. Phys.*, **vol. 62**, 3123-3129, (1987)
[5] L.J. Overzet and J.T. Verdeyen, *Appl. Phys. Lett.*, **vol. 48**, 965, (1986)
[6] Y. Watanabe, M. Shiratani, S. Matsuo and H. Makino, presented at the *9th ISPC, Pugnoschiuso*, (1989)
[7] G.L. Antokol'ski, *Instrum. Exper. Tech.*, **vol. 4**, 1113-1114, (1970)
[8] N. Sato and H. Tagashira, *IEEE Trans. of Plasma Science*, **vol. 19**, 102-112, (1991)